Long-range dielectric-loaded surface plasmon-polariton waveguides

Tobias Holmgaard,[1,*] **Jacek Gosciniak,**[2] **and Sergey I. Bozhevolnyi**[2]

[1]*Department of Physics and Nanotechnology, Aalborg University, Skjernvej 4A, DK-9220, Aalborg Øst, Denmark*

[2]*Institute of Sensors, Signals and Electrotechnics (SENSE), University of Southern Denmark, Niels Bohrs Allé 1, DK-5230 Odense M, Denmark*

[*]*holmgaard@nano.aau.dk*

Abstract: A waveguiding configuration for surface plasmon polaritons (SPPs) featuring simultaneously a tight mode confinement and long propagation (several millimeters) at telecom wavelengths is proposed and analyzed using the finite-element method. The configuration represents a long-range dielectric-loaded SPP waveguide (LR-DLSPPW), in which a thin and narrow metal stripe is sandwiched between a square dielectric ridge and a dielectric film supported by a low-index substrate. Considering optical polymers, for example, we calculated that a 15-nm-thick and 500-nm-wide gold stripe placed on a 460 nm thick medium-index (1.49) layer supported by a low-index (1.34) substrate and topped by a 850×850 nm^2 high-index (1.535) ridge supports a fundamental LR-DLSPPW mode having width of 1.6 μm and propagating over 3.1 mm at the wavelength $\lambda = 1.55$ μm. The proposed configuration allows for easy connection to electrodes enabling, e.g., thermo- or electro-optic control, and is technologically simple being compatible with planar fabrication using UV-lithography.

OCIS codes: (240.6680) Surface plasmons; (130.3120) Integrated optics devices; (130.5460) Polymer waveguides.

References and links

1. D. K. Gramotnev and S. I. Bozhevolnyi, "Plasmonics beyond the diffraction limit," Nat. Photonics **4**, 83–91 (2010).
2. S. Lal, S. Link, and N. J. Halas, "Nano-optics from sensing to waveguiding," Nat. Photonics **1**, 641–648 (2007).
3. H. Raether, *Surface Plasmons on Smooth and Rough Surfaces and on Gratings* (Springer-Verlag, Berlin, 1988), 1st ed.
4. W. L. Barnes, A. Dereux, and T. W. Ebbesen, "Surface plasmon subwavelength optics," Nature **424**, 824–830 (2003).
5. J. Takahara, S. Yamagishi, H. Taki, A. Morimoto, and T. Kobayashi, "Guiding of a one-dimensional optical beam with nanometer diameter," Opt. Lett. **22**, 475 (1997).
6. M. Quinten, A. Leitner, J. R. Krenn, and F. R. Aussenegg, "Electromagnetic energy transport via linear chains of silver nanoparticles," Opt. Lett. **23**, 1331 (1998).
7. I. V. Novikov and A. A. Maradudin, "Channel polaritons," Phys. Rev. B **66**, 035403 (2002).
8. P. Berini, "Plasmon-polariton waves guided by thin lossy metal films of finite width: Bound modes of symmetric structures," Phys. Rev. B **61**, 10484 (2000).
9. C. Reinhardt, S. Passinger, B. N. Chichkov, C. Marquart, I. P. Radko, and S. I. Bozhevolnyi, "Laser-fabricated dielectric optical components for surface plasmon polaritons," Opt. Lett. **31**, 1307–1309 (2006).
10. B. Steinberger, A. Hohenau, H. Ditlbacher, A. L. Stepanov, A. Drezet, F. R. Aussenegg, A. Leitner, and J. R. Krenn, "Dielectric stripes on gold as surface plasmon waveguides," Appl. Phys. Lett. **88**, 094104 (2006).

#133876 - $15.00 USD Received 24 Aug 2010; revised 10 Oct 2010; accepted 12 Oct 2010; published 15 Oct 2010

11. A. Boltasseva, T. Nikolajsen, K. Leosson, K. Kjaer, M. S. Larsen, and S. I. Bozhevolnyi, "Integrated optical components utilizing long-range surface plasmon polaritons," J. Lightwave Technol. **23**, 413 (2005).
12. T. Holmgaard, Z. Chen, S. I. Bozhevolnyi, L. Markey, A. Dereux, A. V. Krasavin, and A. V. Zayats, "Wavelength selection by dielectric-loaded plasmonic components," Appl. Phys. Lett. **94**, 051111 (2009).
13. T. Nikolajsen, K. Leosson, and S. I. Bozhevolnyi, "Surface plasmon polariton based modulators and switches operating at telecom wavelengths," Appl. Phys. Lett. **85**, 5833–5835 (2004).
14. J. Gosciniak, S. I. Bozhevolnyi, T. B. Andersen, V. S. Volkov, J. Kjelstrup-Hansen, L. Markey, and A. Dereux, "Thermo-optic control of dielectric-loaded plasmonic waveguide components," Opt. Express **18**, 1207–1216 (2010).
15. I. D. Leon and P. Berini, "Amplification of long-range surface plasmons by a dipolar gain medium," Nat. Photonics **4**, 382–387 (2010).
16. M. C. Gather, K. Meerholz, N. Danz, and K. Leosson, "Net optical gain in a plasmonic waveguide embedded in a fluorescent polymer," Nat. Photonics **4**, 457–461 (2010).
17. J. Grandidier, G. C. des Francs, S. Massenot, A. Bouhelier, L. Markey, J.-C. Weeber, C. Finot, and A. Dereux, "Gain-assisted propagation in a plasmonic waveguide at telecom wavelength," Nano Lett. **9**, 2935–2939 (2009).
18. T. Holmgaard and S. I. Bozhevolnyi, "Theoretical analysis of dielectric-loaded surface plasmon-polariton waveguides," Phys. Rev. B **75**, 245405 (2007).
19. Y. Binfeng, H. Guohua, and C. Yiping, "Bound modes analysis of symmetric dielectric loaded surface plasmon-polariton waveguides," Opt. Express **17**, 3610–3618 (2009).
20. J. Chen, Z. Li, S. Yue, and Q. Gong, "Hybrid long-range surface plasmon-polariton modes with tight field confinement guided by asymmetrical waveguides," Opt. Express **17**, 23603–23609 (2009).
21. A. V. Krasavin and A. V. Zayats, "Three-dimensional numerical modeling of photonic integration with dielectric-loaded spp waveguides," Phys. Rev. B **78**, 045425 (2008).
22. J. J. Burke, G. I. Stegeman, and T. Tamir, "Surface-polariton-like waves guided by thin, lossy metal films," Phys. Rev. B **33**, 5186–5201 (1986).
23. E. D. Palik, *Handbook of Optical Constants of Solids* (Academic, New York, 1985), 1st ed.
24. J. K. S. Poon, L. Zhu, G. A. DeRose, and A. Yariv, "Transmission and group delay of microring coupled-resonator optical waveguides," Opt. Lett. **31**, 456–458 (2006).
25. R. F. Oulton, G. Bartal, D. F. P. Pile, and X. Zhang, "Confinement and propagation characteristics of subwavelength plasmonic modes," N. J. Phys. **10**, 105018 (2008).
26. T. Holmgaard, Z. Chen, S. I. Bozhevolnyi, L. Markey, and A. Dereux, "Design and characterization of dielectric-loaded plasmonic directional couplers," J. Lightwave Technol. **27**, 5521–5528 (2009).

1. Introduction

Photonic components based on surface plasmon polaritons (SPPs) have attracted great attention in recent years promising to combine large operational bandwidth of photonics with high-density integration achievable in plasmonics [1, 2]. SPPs are electromagnetic waves coupled to collective oscillations in the surface plasma of a metal [3]. SPPs feature a field maximum at a metal-dielectric interface and decay exponentially away from it thus exhibiting a strong intrinsic confinement in the direction perpendicular to the interface [4]. Several different waveguiding configurations support SPP modes confined laterally below the diffraction limit, e.g., metallic nanowires [5], chains of nanospheres [6], and channels cut into a metal [7]. One of the challenges shared by all subwavelength plasmonic structures is considerable propagation losses (due to absorption by the metal involved) that increase drastically for better confined modes. The metal present in SPP waveguides introduces losses, but at the same time it is one of the greatest virtues of plasmonics as it enables easy access to external electrodes and thus offers the possibility of inducing, e.g., thermo- or electro-optic effects in the waveguide components. Thus the possibility of achieving subwavelength mode confinement is not the only argument for considering SPP waveguides, as the presence of a metal electrode right where the SPP field is at its maximum greatly enhances the sensitivity to an applied signal. The absorption losses can, however, be reduced by using long-range SPP (LR-SPP) waveguides, where the longitudinal component of the electric field in the metal, responsible for the absorption losses, is sought minimized [8]. In this work an LR-SPP waveguide configuration based on dielectric-loaded SPP waveguides (DLSPPWs) [9, 10] is proposed and studied using two-dimensional finite-element method (FEM) simulations. The LR-SPP and DLSPP waveguide configurations

#133876 - $15.00 USD Received 24 Aug 2010; revised 10 Oct 2010; accepted 12 Oct 2010; published 15 Oct 2010

have so far, as the only SPP waveguides, demonstrated the realization of complex circuit elements [11, 12], active control by thermo-optic modulation [13, 14], and even loss compensation using optical pumping [15–17], thus confirming the potential of these plasmonic waveguides as a new chip technology with diverse applications. In DLSPPWs, mode confinement is achieved by employing a dielectric ridge deposited on a smooth metal film [18]. The DLSPPW structure is very attractive as a plasmonic waveguide by being versatile with respect to the choice of dielectric, exhibiting, e.g., thermo-optic coefficient, and due to ease of fabrication using industry compatible lithography techniques [14]. By reducing the size of the underlying metal film, i.e., making it a thin stripe, and by employing a dielectric material below the metal film the propagation losses can be reduced significantly [19, 20]. However, in realizing LR-DLSPPWs one must be very careful not to endanger some of the assets of the DLSPPW technology as seen in [19,20], especially in regard to ease of fabrication and the possibility of using the same metal strips for both guiding SPP modes and transmitting electrical signals controlling this guidance. Low propagation losses, ease of fabrication, and possibility to incorporate active elements, e.g., by electro-optic control, are the key advantages of the proposed LR-DLSPPW structure, which makes it a promising plasmonic waveguide structure with the potential of realizing circuits with various functionalities.

2. Waveguide configuration

The proposed long-range plasmonic waveguide is, unlike previous studies of DLSPPWs [18, 21], based on a metal film of finite width, i.e., a metal stripe, and can thus be considered a hybrid plasmonic waveguide. The LR-DLSPPW configuration consists of a dielectric ridge deposited on top of a thin metal stripe which is supported by a dielectric film (Fig. 1). The entire structure is supported by a low-index substrate which ensures mode confinement to the dielectric ridge and underlying dielectric film. Due to the thin metal film, the SPPs on

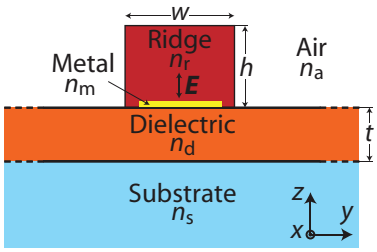

Fig. 1. (Color online) Layout of the LR-DLSPPW structure, with a dielectric ridge on top of a thin metal stripe deposited on an underlying dielectric layer supported by a low-index glass substrate.

the two metal-dielectric interfaces couple to each other and form supermodes with symmetric and anti-symmetric transverse component (E_z) [22]. The symmetric mode is often denoted the long-range mode as the longitudinal component of the electric field (E_x) in the metal is minimized thus lowering the absorption losses. Hereby the LR-DLSPPW structure suggested here allows one to significantly suppresses the propagation losses while retaining a strong mode confinement as well as to straightforwardly connect SPP guiding metal stripes with external electrodes using planar fabrication.

The LR-DLSPPW configuration is analyzed using FEM simulations at the telecom wavelength of 1.55 μm, and in the following, the width of metal stripe is 500 nm and its thickness is 15 nm unless stated otherwise. We have chosen to consider a benzocyclobutene (BCB) ridge $(n_r = 1.535)$ [11] placed on a gold stripe $(n_m = 0.55 + i11.5)$ [23] supported by a poly-methyl-

#133876 - $15.00 USD Received 24 Aug 2010; revised 10 Oct 2010; accepted 12 Oct 2010; published 15 Oct 2010

methacrylate (PMMA) film ($n_d = 1.493$) [24] and a Cytop substrate ($n_s = 1.34$) [24], but other transparent dielectric materials can also be used as long as the substrate features a sufficiently low refractive index in the wavelength range of interest. We found that the considered configuration indeed supports a well confined symmetric mode with low propagation losses at telecom wavelengths (Fig. 2). A field profile of the transverse component of the electric field taken

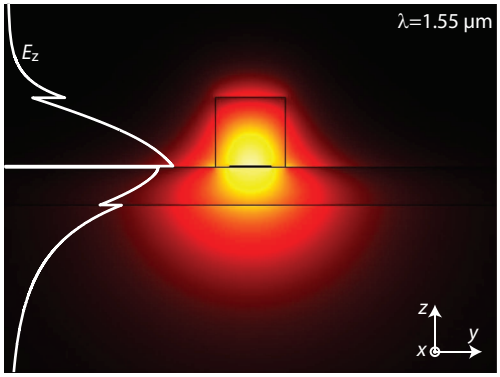

Fig. 2. (Color online) Field distribution of abs(E_z) in the cross-section of the LR-DLSPPW with the parameters $h = 850$ nm, $w = 850$ nm, and $t = 460$ nm. Insert shows a vertical profile of E_z through the center of the ridge.

through the middle of the waveguide confirms that the mode is the symmetric long-range mode, in this case exhibiting a mode effective index $N_{eff} = 1.37$ and a propagation length $L = 3.1$ mm. It is observed that the mode field is maximized close to the metal stripe, promising a high sensitivity to any changes, e.g., thermo-optic, induced by the metal stripe.

3. Propagation characteristics and mode confinement

In order to minimize the propagation losses, the mode field on either side of the metal strip must be balanced, which is done by varying the thickness of the PMMA layer (Fig. 3). For a

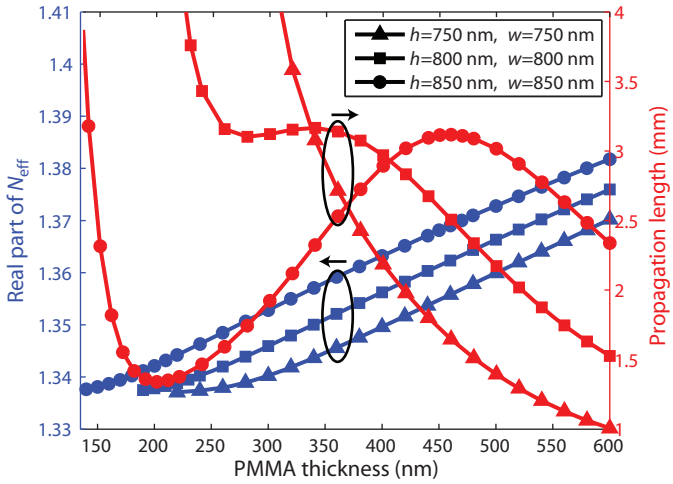

Fig. 3. (Color online) Real part of the mode effective index and the propagation length versus thickness of the PMMA layer for two different ridge dimensions.

#133876 - $15.00 USD Received 24 Aug 2010; revised 10 Oct 2010; accepted 12 Oct 2010; published 15 Oct 2010

square ridge of dimensions $h = 850$ nm, $w = 850$ nm a local maximum in the propagation length ($L = 3.1$ mm) is observed at the thickness $t = 460$ nm, corresponding to the well confined mode ($N_{\text{eff}} = 1.37$) shown in the field plot above (Fig. 2). Decreasing the thickness of the PMMA layer initially has the effect of breaking the symmetry in the mode field distribution in depth, thus causing the propagation length to drop until the thickness where the mode reaches cutoff ($N_{\text{eff}} = 1.34$) and the mode becomes a dielectric optical mode in the Cytop substrate. Increasing the PMMA thickness similarly breaks the symmetry, thus increasing the longitudinal (dominant) electric field component inside the metal film, which causes an increase in the absorption and decrease in the propagation length. Increasing the PMMA thickness further ($t \sim 900$ nm) the waveguide structure becomes multi-mode as a photonics mode starts to be supported in the dielectric layer. For smaller ridge dimensions ($h = 800$ nm, $w = 800$ nm) the local maximum and cutoff point are closer and the maximum in the propagation length is less pronounced (Fig. 3). For even smaller ridge dimensions ($h = 750$ nm, $w = 750$ nm) the PMMA thickness ensuring symmetry of the mode field yields a mode effective index below 1.34, i.e., below the cutoff, and thus no local maximum in the propagation exist as it is not possible to minimize the longitudinal component of the electric field in the metal. This implies that the propagation length decreases monotonously with an increase in thickness of the dielectric layer (Fig. 3).

The lateral mode confinement, which is important when realizing both passive and active components (as it is the lateral mode width which determines the minimum bend radius achievable without introducing large bend losses), is expected to increase rapidly for small PMMA thicknesses as the mode starts to spread in the Cytop substrate. For large PMMA thicknesses the mode in the PMMA film resembles that of an optical TM mode in the film, with field maximum in the middle of the film and decreasing lateral confinement. Thus the LR-DLSPPWs feature a minimum of the mode size at a certain thickness of the dielectric. Calculations of the lateral mode width versus PMMA thickness confirms this trend, and reveals that for a $h = 850$ nm, $w = 850$ nm ridge the minimum appears at $t = 400$ nm with the value 1.64 μm [Fig. 4(a)]. Due

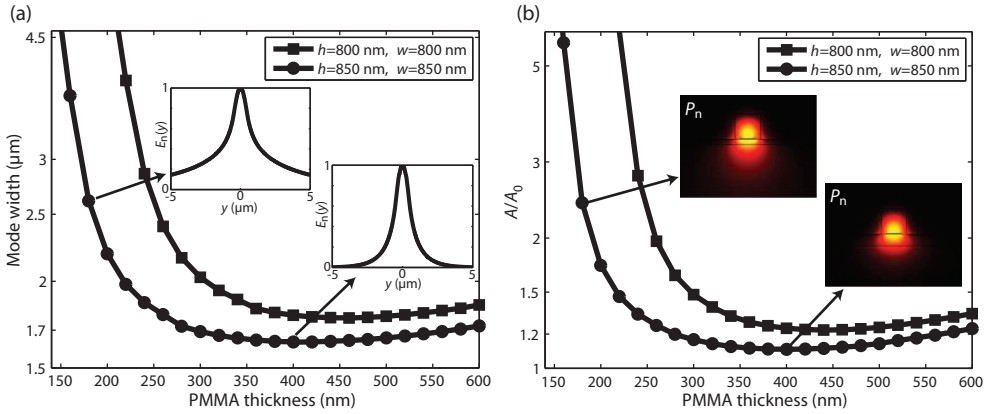

Fig. 4. (Color online) (a) Mode width (log scale) versus thickness of the PMMA layer for the ridge dimensions $h = 800$ nm, $w = 800$ nm and $h = 850$ nm, $w = 850$ nm. The insets show $E_{\text{n}}(y)$ at $t = 180$ nm and $t = 400$ nm. (b) Normalized effective mode area (log scale) versus thickness of the PMMA layer for same ridge dimensions as in (a). The insets show the norm of the power flow at $t = 180$ nm and $t = 400$ nm.

to the smaller mode effective index of a $h = 800$ nm, $w = 800$ nm ridge one expects, and indeed observes, a weaker mode confinement in this case [Fig. 4(a)]. The lateral mode widths are found by taking the width of the norm of the electric field $E_{\text{n}}(y)$ at $1/e$ of its maximum value, where $E_{\text{n}}(y)$ is calculated by integrating $E_{\text{n}}(y,z)$ over z in the entire computational window. Since there

#133876 - $15.00 USD Received 24 Aug 2010; revised 10 Oct 2010; accepted 12 Oct 2010; published 15 Oct 2010

are no rapid variations in the mode field distribution of the LR-DLSPPW structure (Fig. 2) the determined mode widths are directly comparable to lateral mode widths of other plasmonic structures. Furthermore, calculations of the widely used normalized mode effective area A/A_0 [Fig. 4(b)], A being the mode area encompassing half the mode power and $A_0 = (\lambda/2)^2$ being the diffraction limited area of vacuum, have also been performed to allow direct comparison with other plasmonic waveguides [25]. The investigated LR-DLSPPW configuration features a normalized mode effective area close to 1 [Fig. 4(b)], combined with normalized propagation distance $L/\lambda \sim 2000$ (Fig.3), thus demonstrating the potential of the waveguide structure. As in any waveguide configuration there is a limit to the integration of components due to possible crosstalk between adjacent waveguides. A direct investigation of this has been performed by considering coupling between two identical adjacent waveguides using the supermode approach [26]. The results show that when increasing the center-to-center separation between two adjacent LR-DLSPPWs from 4 μm to 6 μm, the coupling length increases more than 10 times from about half the propagation length to more than 5 times the propagation length, more than enough to ensure isolation. The fact that directional couplers based on LR-SPP waveguides have center-to-center separation in the order of $10-15$ μm [11] confirms that the considered LR-DLSPPW modes are significantly better confined than the LR-SPP waveguide modes.

From the above, it is observed that by shrinking the size of the ridge, one must also shrink the thickness of the sublayer in order to balance the mode field on either side of the metal strip, thus minimizing the propagation losses. Similarly a decrease in the refractive index of a ridge should be balanced by its size or by a decrease in the thickness of the sublayer.

4. Metal stripe dependence

The dependence of the mode effective index and propagation length on the width of the metal stripe is investigated for a square ridge ($h = 850$ nm, $w = 850$ nm) and 460 nm thick dielectric layer (Fig. 5). When increasing the width of the metal stripe, keeping all other parameters

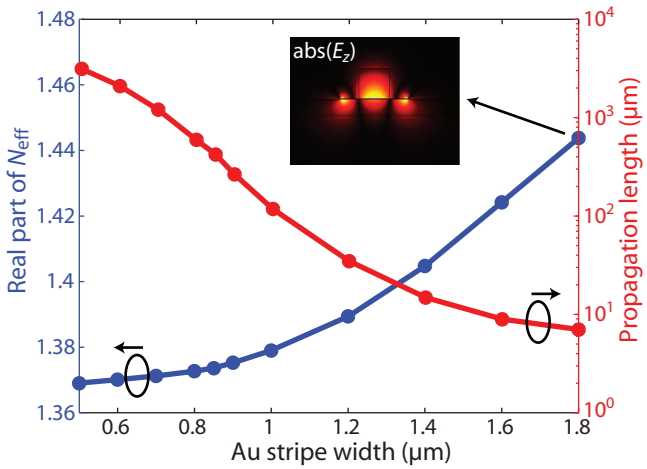

Fig. 5. (Color online) The dependence of the real part of the mode effective index and the propagation length (log scale) on the width of the Au stripe for the BCB ridge dimensions $h = 850$ nm, $w = 850$ nm, and thickness of the PMMA layer $t = 460$ nm. The insert shows the field distribution at a stripe width of 1.8 μm

constant, the mode effective index increases, and the propagation length decreases due to the larger area inside the ridge covered with the metal, which accounts for the absorption losses.

#133876 - $15.00 USD Received 24 Aug 2010; revised 10 Oct 2010; accepted 12 Oct 2010; published 15 Oct 2010

At the point when the width of the metal stripe exceeds that of the ridge a new regime enters, which essentially can be described as a three domain waveguide structure consisting of the ridge region, and the surrounding four layer (air-metal-dielectric-substrate) regions, surrounding the ridge on either side. The TM mode (SPP) supported in the surrounding regions is asymmetric with a mode effective index of ~ 1.5, much higher than that in the ridge region, and with much larger propagation losses. This implies that for increasing width of the metal stripe the guiding properties will be dominated by the characteristics of the surrounding regions, which give rise to increasing mode effective index and rapidly decreasing propagation length with stripe width (Fig. 5). This entails that it is desirable to keep the width of the metal stripe equal to or smaller than the width of the ridge. A further decrease of the width of the metal stripe implies that the LR-DLSPPW mode approaches the TM optical mode supported by the dielectric materials, with a mode effective index slightly above 1.36. Due to practical considerations related to the fabrication and interfacing to external electrodes one should be careful, however, to decrease the width of the stripe much below 500 nm. Similar reasoning can be applied in regard to choice of metal stripe thickness. When altering the thickness of the metal stripe, the propagation losses change significantly, in favor of thinner metal stripes, however, the mode confinement does not change accordingly. For example increasing the thickness from 15 nm to 30 nm (keeping all other parameters constant) changes the propagation length from 3.1 mm to 0.67 mm, but only decreases the lateral mode width by 6%. Again practical considerations and fabrication capabilities set the lower boundary for the stripe thickness, partly due to the lower limit for smooth Au deposition [11], but also considering that, when realizing active components, the metal stripes will be utilized as electrodes, which imply that their thickness need to be large enough to ensure their mechanical and electrical stability, i.e., for making stable contacts and avoiding overheating in defects.

5. Conclusion

In conclusion a long-range waveguide based on DLSPPWs for guiding plasmonic modes over several millimeters at telecom wavelengths, while retaining strong mode confinement, has been proposed and investigated using FEM simulations. The structure consists of a dielectric ridge deposited on top of a thin metal stripe, supported by a dielectric layer and a substrate. A LR-DLSPPW with a propagation length of 3.1 mm and a lateral mode width of 1.6 μm is demonstrated. The structure features easy access to external electrodes as the metal stripe supporting the LR-DLSPPW modes rests on a smooth dielectric film and can be fabricated using standard lithography techniques. In addition to this, the compatibility with polymers with various active properties makes the proposed structure very promising when seeking to realize efficient active plasmonic components.

Acknowledgments

This work was supported by EC-ICT FP7 PLATON and by FTP-project No. 09-072949 ANAP.

#133876 - $15.00 USD Received 24 Aug 2010; revised 10 Oct 2010; accepted 12 Oct 2010; published 15 Oct 2010